Optical Materials 35 (2012) 56–60

Contents lists available at SciVerse ScienceDirect

Optical Materials

journal homepage: www.elsevier.com/locate/optmat

Transparent UV-absorbers thin films of zinc oxide: Ceria system synthesized via sol–gel process

Juliana Fonseca de Lima, Renata Figueredo Martins, Osvaldo Antonio Serra *

Department of Chemistry, FFCLRP, USP, Avenida Bandeirantes 3900, CEP 14040-901, Ribeirão Preto, SP, Brazil

ARTICLE INFO

Article history:
Received 9 March 2012
Received in revised form 20 June 2012
Accepted 27 June 2012
Available online 26 July 2012

Keywords:
CeO_2
ZnO
UV-protective coatings
Sol–gel

ABSTRACT

Transparent nanostructure ZnO:CeO_2 and ZnO thin films to use as solar protector were prepared by non-alkoxide sol–gel process and deposited on boronsilicate glass substrate by dip-coating technique and then heated at 300–500 °C. The films were characterized structurally, morphologically and optically by X-ray diffraction (XRD), atomic force microscopy (AFM), field emission gun-scanning electron microscopy (FEG-SEM), scanning electron microscopy (SEM) and UV–Vis transmittance spectroscopy. The coatings presented high transparency in the visible region and excellent absorption in the UV. The band gap of the deposited films was estimated between 3.10 and 3.18 eV. Absorption of the films in the UV was increased by presence of cerium. The results suggest that the materials are promising candidates to use as coating solar protective.

1. Introduction

The need to use UV absorbers, organics and inorganics, to protect material that has been exposed to the solar radiation has motivated numerous studies about the synthesis and properties of these absorbers. They have been most frequently used in cosmetics to prevent sunburns and skin cancer [1], in glass, polymers, and wooden substrates, maintaining the integrity of their physical–chemical properties.

Organic UV absorbers have been widely used as coatings to protect organic materials against UV radiation. UVA (benzophenones, anthranilates and dibenzoylmethanes) and UVB absorbers (PABA derivatives, salicylates, cinnamates and camphor derivatives) are utilized combined to cover the whole UVA/UVB range (290–400 nm) [2]. Their properties as light in weight, resistant to corrosion, relatively easily fabricated at moderate temperatures and low cost of the starting materials are the most important reasons for their wide utilization. However, their applications sometimes are limited due to their sensibility to heat and self photo-degradation leading to a low effective lifetime and the formation of another substances UV non-absorbers.

Inorganic materials have been extensively utilized in sunscreen products due to the efficient absorption in the UVA and UVB region. Inorganic or nonchemical sunscreen filters, titania (TiO_2) and zinc oxide (ZnO) are effective inorganic sunscreens and commonly used nowadays [3–5]. The morphology of these compounds is very important to determine the utilization of them as absorbers in the UVA and UVB region. For instance, amorphous ZnO and TiO_2 have a much higher band gap than the respective crystalline phases showing its absorption, displaced to lower wavelengths, does not cover the whole UV region of interest. Ceria (CeO_2) has potential interest as an inorganic UV blocking material. Many studies have reported the synthesis of nano-sized particles of ceria undoped and doped for several applications [6–9]. Some of their properties as: being obtained as crystalline or amorphous forms at low temperatures with similar band gaps near to 3.1 eV (about 400 nm) [10]; refractive index of CeO_2 in the visible region is 2.1–2.2 [11], almost the same as that of ZnO (2.0–2.1) [12], become it a very attractive material to be utilized as UV absorbers.

Sol–gel methodology has been extensively used in order to synthesize inorganic materials, because it requires very simple equipments, allows the use of different precursors and soft conditions [13]; also the sol–gel method is a simple, low cost and large area coating method [14]. Some studies have been reported in obtaining UV absorber films used the sol–gel process, for example, in the synthesis of composites of TiO_2–CeO_2–SiO_2 and CeO_2–SiO_2 [15], silica-coated TiO_2 [16]. However, none of these studies relate the synthesis and characterization of composites of the ZnO:CeO_2 using the sol–gel process for applications as UV filter for coatings. The system ZnO:CeO_2 become a potential UV absorber with desired properties as wide band gap, optical transparence in the visible region, transparent coating in high temperature and good heat resistance. These good properties allow to apply the ZnO:CeO_2 in optical materials [14,15]. In this study, ZnO:CeO_2 films have been synthesized by the sol–gel process using non-alkoxide route [17].

* Corresponding author. Tel.: +55 16 3602 3746.
E-mail address: osaserra@usp.br (O.A. Serra).

0925-3467/$ - see front matter © 2012 Elsevier B.V. All rights reserved.
http://dx.doi.org/10.1016/j.optmat.2012.06.016

2. Experimental procedures

In this experiment, a similar procedure as described in [18,19] is performed. Zinc acetate dihydrate and cerium nitrate are used as starting materials sources, ethanol and lactic acid were used as solvent and stabilizer, respectively. Zinc acetate dihydrate was added to ethanol ($[Zn^{2+}] = 0.44$ mol L^{-1}) and later mixed with an ethanolic solution of cerium nitrate (0.10 mol L^{-1}) in appropriated stoichiometry (Zn^{2+}:Ce^{3+} = 9:1). The solution was heated under reflux for 3 h at 70 °C with additions of lactic acid to stabilize the sol, the flask was fitted with a condenser and a trap ($CaCl_2$) to avoid moisture exposure. Stable and translucent colloidal precursor sol has been obtained. The films were deposited over borosilicate glass substrates previously cleaned with a sodium dodecylsulfate detergent, treated ultrasonically with deionized water for 30 min [20]. Transfer process onto glass substrates was carried out by dip-coating at 4.0 cm min^{-1} with a short immersion time (30 s). The films were then annealed to temperatures of 300, 400 and 500 °C during 15 min. The coating procedure was repeated five times to each temperature. ZnO films were obtained utilizing the same procedure as described previously. In Fig. 1 are the final films ZnO (500 °C) and ZnO:CeO_2 (500 °C), the coatings show very high transparency.

The sample crystallographic characterization was performed by X-ray diffraction (XRD) in a Siemens D5000 diffractometer equipped with Cu Kα radiation. ZnO and ZnO:CeO_2 crystallite size was determined by Scherrer equation [21]. The UV absorption capacity of the films was analyzed by absorption spectra from 280 to 700 nm that were measured in a spectrometer HP 8453 Diode Array. The morphologies and cross-sections were investigated respectively by field emission gun-scanning electron microscopy (FEG-SEM) on a Quanta 200 FEG – FEIelectron microscopy that were performed in the Center of Microscopy at Universidade Federal de Minas Gerais, Belo Horizonte, MG, Brazil (http://www.microscopia.ufmg.br), and a scanning electron microscopy (SEM) on a Scanning Electron Microscope Zeiss EVO 50. The surface roughness and also morphology of ZnO:CeO_2 (500 °C) were measured with a Nanoscope III atomic force microscope (Digital Co. Instruments, USA) using a normal silicon nitride tip (Xμm) in Tapping Mode scanning the surface with an oscillating tip to its resonant frequency (200–400 kHz).

3. Results and discussion

In Fig. 2 is the XRD pattern of the film calcined at 500 °C. The interplanar distances observed are related to the CeO_2 phases, fluorite-type, face-centered cubic unit cell and space group Fm3m (225) or ZnO phases, hexagonal system, primitive unit cell and space group P63mc (186) [22], however the display peaks for the ZnO is sharper, once CeO_2 is presented in the range of 10%.

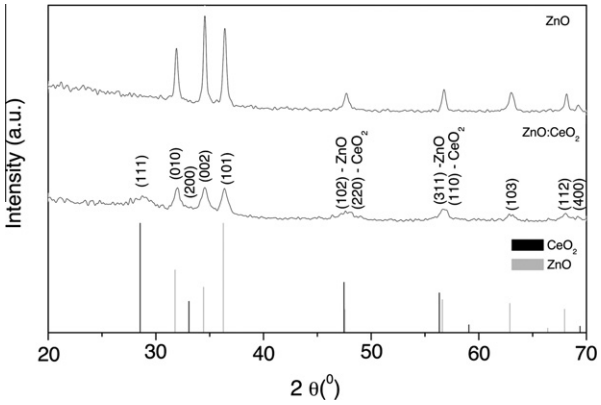

Fig. 2. X-ray diffraction patterns of ZnO and ZnO:CeO_2 films annealed at 500 °C.

The average crystallite size of the particles on the films was calculated by Scherrer's Formula [21] and the estimated values are in Table 1. The average crystallite sizes for ZnO and ZnO:CeO_2 were 25.1 and 19.8 nm. The average crystallite sizes show a minimal decreased with cerium presence.

Fig. 3 shows the UV–Vis spectra of the films of ZnO. The films thermally treated at 400 and 500 °C presented high absorption in the 290–400 nm region and good transparency in the visible (400–700 nm), while the obtained at 300 °C presented very low UV absorption because in this case does not happen the formation of zinc oxide. The UV absorption increased linearly with the thickness of the films obtained by dip-coating process. The films treated at 500 °C presented a more intense absorption between 300 and 400 nm due to a higher crystallinity of the ZnO phase, as showed in the XRD patterns, Fig. 2.

The ZnO:CeO_2 thin films treated at 300, 400 and 500 °C, exhibit efficient absorption in the 290–400 nm region and a good transparency in the visible (400–700 nm), with a negligible yellowish coloration from the CeO_2 (Fig. 4). As observed for the ZnO, the absorption increased with the thickness and the temperature treatment of the films. Due to the formation of crystalline phase of CeO_2 at low temperature (300 °C), the films of the composites ZnO:CeO_2 present high absorption even at 300 °C. The presence of CeO_2 imply in higher absorption in the 290–400 nm region than the films containing only ZnO (Figs. 3 and 4).

The good transmission in the visible region and good absorption in the UV region corresponds to the ideal band gap of the films. The Tauc Plot [23] is commonly used to determine the optical band gap in thin film materials by the following equation:

$$(\alpha h\nu) = A(h\nu - \mathrm{Eg})^n \quad (1)$$

where α is the absorption coefficient, $h\nu$ is the photon energy and Eg is the optical band gap. The optical absorption coefficient α can be calculated from the equation:

$$\alpha d = \ln(1/T) \quad (2)$$

where T is the transmittance and d is the thickness of the films.

The optical band gap was estimated by extrapolating the straight line region in the plot of $(\alpha h\nu)^2$ versus photon energy (Fig. 5), the extrapolated band gap values are 3.10 and 3.18 for ZnO:CeO_2 and ZnO films respectively, these values have relevance in solar protection.

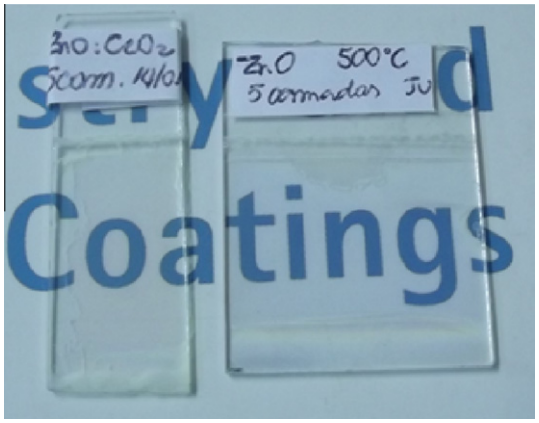

Fig. 1. Photography of the transparent films with five layers and treated at 500 °C. (1) ZnO:CeO_2 and (2) ZnO.

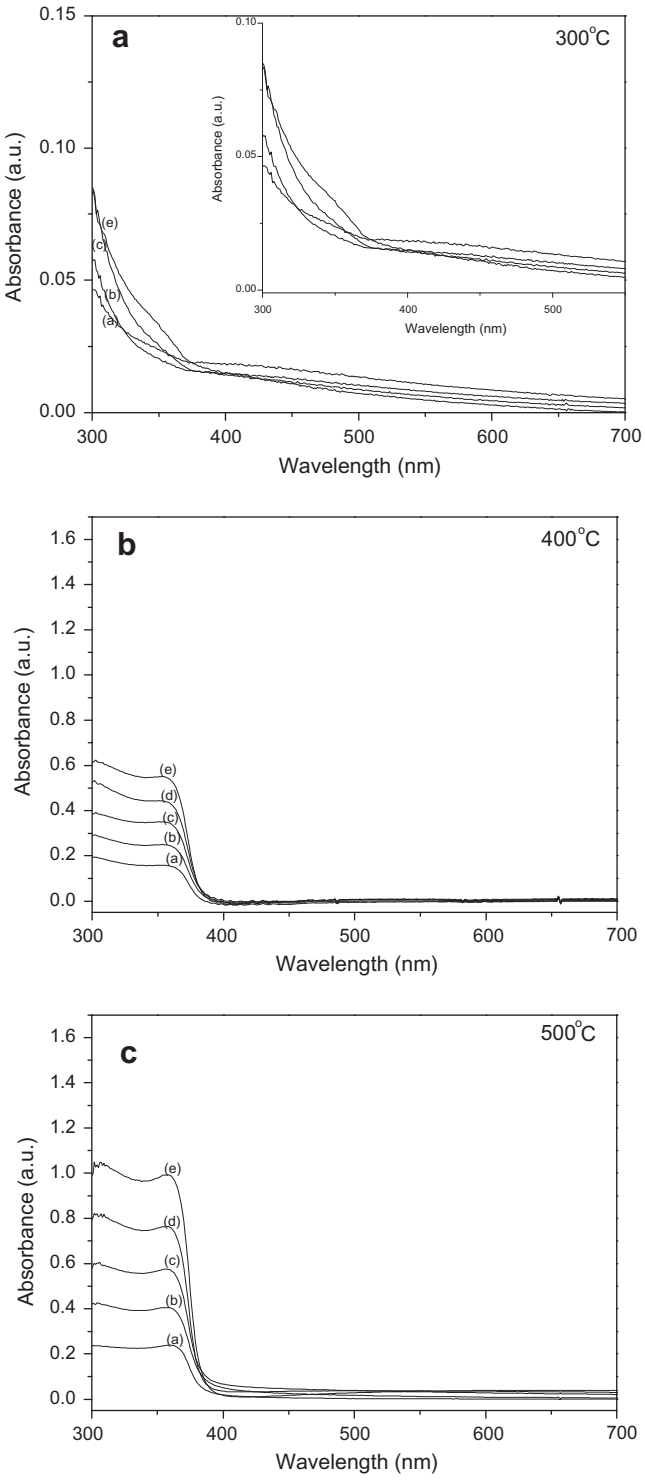

Fig. 3. Absorption spectra of ZnO films annealed at 300, 400 and 500 °C: (a) 1 layer, (b) 2 layers, (c) 3 layers, (d) 4 layers and (e) 5 layers.

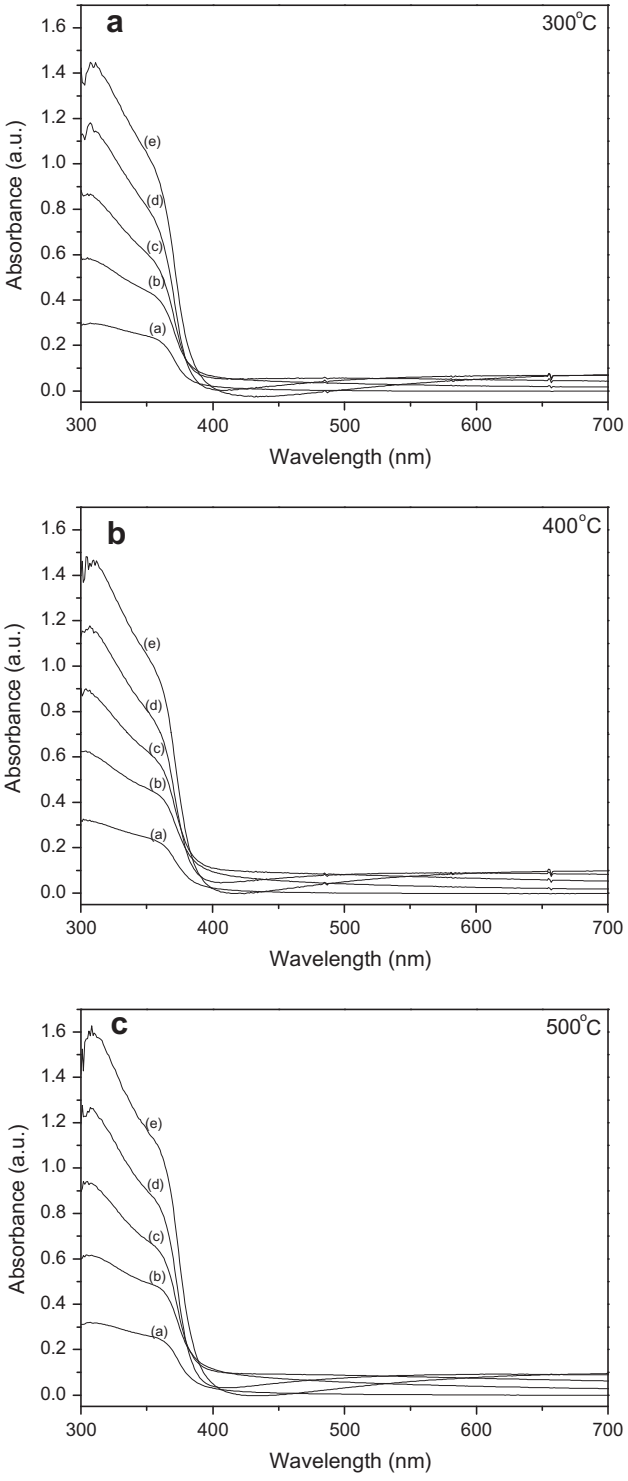

Fig. 4. Absorption spectra of ZnO:CeO_2 films annealed at 300, 400 and 500 °C: (a) 1 layer, (b) 2 layers, (c) 3 layers, (d) 4 layers and (e) 5 layers.

FEG-SEM images in Fig. 6a and b and show the morphological aspects of the thin films ZnO and ZnO:CeO_2 on the surface of the substrate. The deposited films have a granular structure with a size of about 25 nm for ZnO film forming small aggregates (Fig. 6a) and for ZnO:CeO_2 film the particles size have about 50–100 nm for CeO_2 agglomerate that is the white part of the image (Fig. 6b) and it is possible to observe that small particles of ZnO form agglomerates of approximately 125 nm (Fig. 6b). Comparing the particle size to the crystallite size (calculated by X-ray diffraction) for ZnO:CeO_2, it is possible to note a difference in the values due to the formation of nanocrystallite aggregates [24] or agglomerates [24]. It is noteworthy to say that the size of both crystallites and particles are not necessarily the same since the latter may be formed by a number of the former [25].

SEM was used to obtain images to determine, even approximately, the thickness of the films in order to obtain such images was made a cross-section in the substrate. Photomicrographs for the ZnO and ZnO:CeO_2 films with five layers and thermally treated

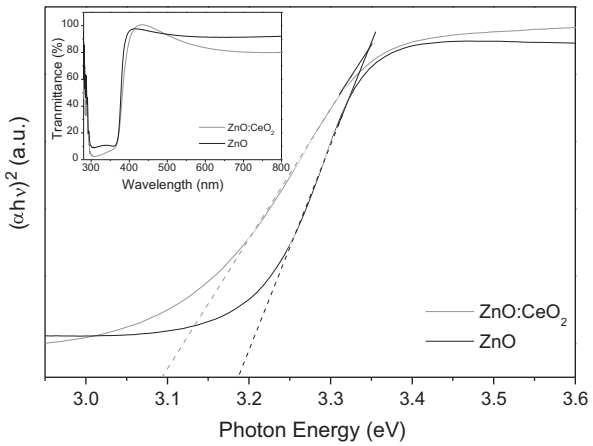

Fig. 5. Plot of $(\alpha h\nu)^2$ versus photon energy and optical transmittance spectra (inside) for ZnO and ZnO:CeO_2 thin films heated at 500 °C.

at 500 °C are shown in Figs. 7a and b. It is observed that the film consists of five layers of ZnO and has a thickness of 126–178 nm (Fig. 7a) and the film formed by the system ZnO:CeO_2 has a thickness of 270–267 nm (Fig. 7b).

The 2D and 3D surface topographies of interested film ZnO:CeO_2 treated at 500 °C obtained by AFM are illustrated in Fig. 8. The films have relatively spherical grains with nanometric dimensions, dense structure and no cracks. In Fig. 8b is shown the difference in roughness that is low. The presence of "mountains" of different sizes is due probably to the formation of two oxides that constitute the studied system, ZnO and CeO_2.

4. Conclusions

ZnO and ZnO:CeO_2 thin films were successfully prepared by non-alkoxide sol–gel method, a simple and low cost method, and deposited on glass substrate by dip-coating. The film thickness could be controlled by the coatings conditions and the solution viscosity. During the synthesis process a stable and translucent colloidal precursor sol was obtained, after transfer process onto glass substrate, transparent films with high UV absorption were obtained and the presence of cerium increased the capacity of the films in absorber the UV range.

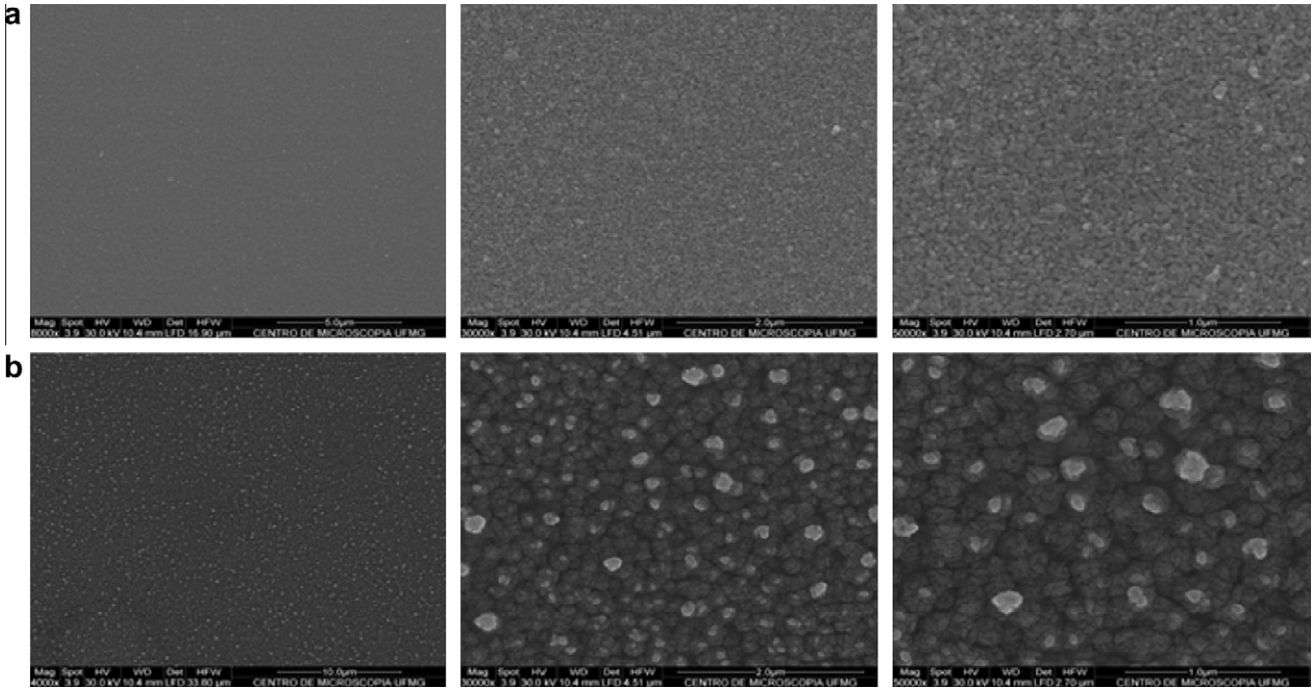

Fig. 6. FEG-SEM images of the surface thin films. (a) FEG-SEM images of ZnO thin film heated at 500 °C. (b) FEG-SEM images of ZnO:CeO_2 thin film heated at 500 °C.

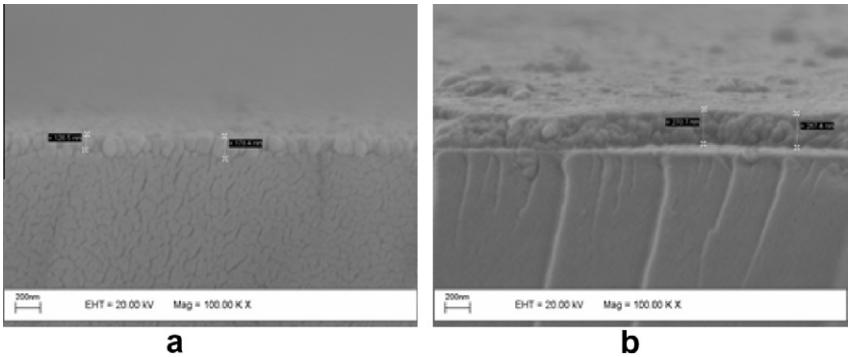

Fig. 7. SEM images of cross-section of the films heated at 500 °C: (a) ZnO and (b) ZnO:CeO_2.

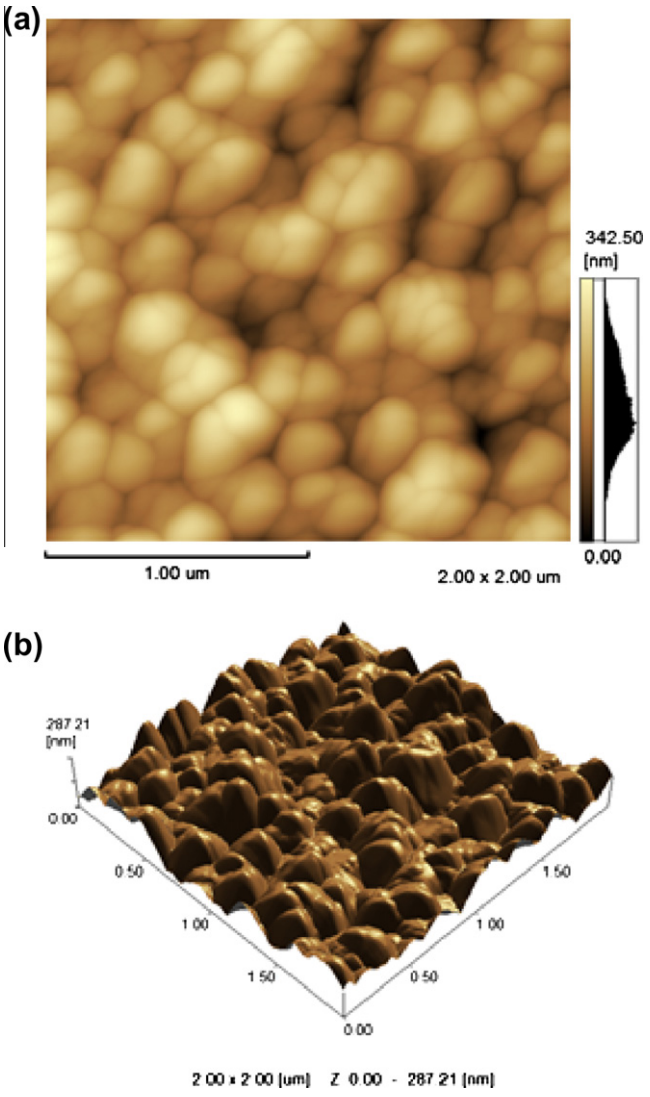

Fig. 8. AFM images of ZnO:CeO_2 thin film treated at 500 °C: (a) 2D image and (b) 3D image.

The final deposited thin films heated at 500 °C were chosen to finish the main analysis. Morphological characterizations showed the formation of nanostructured films with spherical grains, low roughness and no cracks. The band gap values observed for the films were from 3.10 to 3.18 eV and it can be correlated with the nanocrystalline structure of the films and these values also allow the application in solar protection. The results suggest that the materials are promising candidates to use as coating solar protective.

Acknowledgments

We thank Brazilian agencies CAPES, CNPq, and FAPESP for financial support and Grants. We would like to acknowledge the Center of Microscopy at Universidade Federal de Minas Gerais (http://www.microscopia.ufmg.br) for providing the equipment and technical support for experiments involving electron microscopy. We also thanks to Dr. C.M.C do Prado Manso for helpful discussion.

References

[1] T. Maier, H.C. Korting, Skin Pharmacol. Physiol. 18 (2005) 253–262.
[2] S.C. Rastogi, Contact Derm. 46 (2002) 348–351.
[3] S. Livraghi, I. Corazzari, M.C. Paganini, G. Ceccone, E. Giamello, B. Fubini, I. Fenoglio, Chem. Commun. 46 (2010) 8478–8480.
[4] N. Serpone, D. Dondi, A. Albini, Inorg. Chim. Acta 360 (2007) 794–802.
[5] B. Alessio, D. Maximilian, L.N. Pierandrea, P. Piero, J. Nanopart. Res. 10 (2008) 679–689.
[6] S. Yabe, T. Sato, J. Solid State Chem. 171 (2003) 7–11.
[7] M. Toshiyuki, F. Kazuyasu, M. Ken-ichi, A. Gin-ya, Chem. Mater. 9 (1997) 2197–2204.
[8] S. Yabe, M. Yamashita, S. Momose, K. Tahira, S. Yoshida, R. Li, S. Yin, T. Sato, Int. J. Inorg. Mater. 3 (2001) 1003–1008.
[9] Z. Qingna, D. Yuhong, W. Peng, Z. Xiujian, J. Rare Earths 25 (2007) 64–67.
[10] P. Periyat, F. Laffir, S.A.M. Tofail, E. Magner, RSC Adv. 1 (2011) 1794–1798.
[11] K.N. Rao, L. Shivligappa, S. Mohan, Mater. Sci. Eng. B 98 (2003) 38–44.
[12] F.K. Shan, Y.S. Yu, Thin Solid Films 435 (2003) 174–178.
[13] C.J. Brinker, G.W. Scherer, Sol–Gel Science – The Physics and Chemistry of Sol–Gel Processing, Academic Press, London, 1990.
[14] C.-Y. Tsay, H.-C. Cheng, C.-Y. Chen, K.-J. Yang, C.-K. Lin, Thin Solid Films 518 (2009) 1603–1606.
[15] H. Cui, M. Zayat, P.G. Parejo, D. Levy, Adv. Mater. 20 (2008) 65–68.
[16] A. Jaroenworaluck, W. Sunsaneeyametha, N. Kosachan, R. Stevens, Surf. Interface Anal. 38 (2006) 473–477.
[17] J.F. Lima, R.F. Martins, C.R. Neri, O.A. Serra, Appl. Surface Sci. 255 (2009) 9006–9009.
[18] R.F. Silva, M.E.D. Zaniquelli, J. Non-Cryst. Solids 247 (1999) 248–253.
[19] R.F. Silva, M.E.D. Zaniquelli, Thin Solid Films 449 (2004) 86–93.
[20] R.F. Martins, R.F. Silva, R.R. Gonçalves, O.A. Serra, J. Fluoresc. 20 (2010) 739–743.
[21] B. Cullity, Elements of X-ray Diffraction, second ed., Addison-Wesley, Reading, MA, 1978. pp. 447–446.
[22] Powder Diffraction File PDF-2 Database Sets 1–44, Pennsylvania: Joint Committee on Powder diffraction Standards—International Center for Diffraction Data, PDF numbers 75–0390 (CeO2), 80–0074 (ZnO), 1988.
[23] J. Tauc, R. Grigorovici, A. Vancu, Phys. Status Solid 15 (1966) 627–637.
[24] J.G. Darab, J.C. Linehan, D.W. Matson, Energy Fuel. 8 (1994) 1004–1005.
[25] R.B.V. Dreele, Rev. Mineral. Geochem. 63 (2006) 81–98.